



# Analysis of chimney height for solar chimney power plant

Xinping Zhou<sup>a</sup>, Jiakuan Yang<sup>a,\*</sup>, Bo Xiao<sup>a</sup>, Guoxiang Hou<sup>b</sup>, Fang Xing<sup>a</sup>

<sup>a</sup>*School of Environmental Science and Engineering, Huazhong University of Science and Technology, 1037 Luoyu Road, Wuhan, Hubei 430074, PR China*

<sup>b</sup>*School of Traffic Science and Engineering, Huazhong University of Science and Technology, 1037 Luoyu Road, Wuhan, Hubei 430074, PR China*

Received 13 May 2007; accepted 13 February 2008

---

## Abstract

Current in solar chimney power plant that drives turbine generators to generate electricity is driven by buoyancy resulting from higher temperature than the surroundings at different heights. In this paper, the maximum chimney height for convection avoiding negative buoyancy at the latter chimney and the optimal chimney height for maximum power output are presented and analyzed using a theoretical model validated with the measurements of the only one prototype in Manzanares. The results based on the Manzanares prototype show that as standard lapse rate of atmospheric temperature is used, the maximum power output of 102.2 kW is obtained for the optimal chimney height of 615 m, which is lower than the maximum chimney height with a power output of 92.3 kW. Sensitivity analyses are also performed to examine the influence of various lapse rates of atmospheric temperatures and collector radii on maximum height of chimney. The results show that maximum height gradually increases with the lapse rate increasing and go to infinity at a value of around  $0.0098 \text{ K m}^{-1}$ , and that the maximum height for convection and optimal height for maximum power output increase with larger collector radius.

© 2008 Elsevier Ltd. All rights reserved.

*Keywords:* Solar chimney; Maximum height; Optimal height

---

## 1. Introduction

With fossil energy nearing exhaustion as well as greenhouse effect and air pollution being more severe, utilization of renewable energy technologies are increasingly gaining great importance. Solar chimney power technology (see Fig. 1), designed to produce electric power on a large-scale, utilizes solar energy to produce ventilation that drives wind turbines to produce electric power. The technology combines three components: a collector, a chimney and turbines [1]. In the collector, solar radiation is used to heat an absorber (ordinarily soil or water bags) on the ground, and then a large body of air, heated by the absorber, rises up the chimney, due to the density difference of air between the chimney base and the surroundings. The rising air drives large turbines installed at the chimney base to gener-

ate electricity. The concept of solar chimney power technology was first conceived many years ago, again presented in 1978 and proven with the operation of a pilot 50 kW power plant in Manzanares, Spain in the early 1980s [2].

In the recent years, more and more researchers have shown strong interest in studying such solar thermal power generating technology for its huge potential of application all over the world. Four pilot solar chimney power models were in succession built by Krisst [3], Kulunk [4], Pasurmarthi and Sherif [5], Zhou et al. [6]. The researchers also carried out experimental investigations on the performances of the models. More theoretical investigation and simulations have been carried out by Padki and Sherif [7], Lodhi [8], Bernardes et al. [9], Bernardes et al. [10], von Backström and Gannon [11], Gannon and von Backström [12], Pastohr et al. [13], Schlaich et al. [14], Bilgen and Rheault [15], Pretorius and Kröger [16], Ninic [17], Onyango and Ochieng [18].

In order to produce large amount of energy conversion efficiently, a gigantic solar chimney is needed. However, to

---

\* Corresponding author. Tel.: +86 27 87792207; fax: +86 27 87543512.

E-mail addresses: [zhxpmark@hotmail.com](mailto:zhxpmark@hotmail.com) (X. Zhou), [yjiakuan@hotmail.com](mailto:yjiakuan@hotmail.com) (J. Yang).

## Nomenclature

$A_c$	cross section area of chimney ( $m^2$ )	$V$	velocity magnitude ( $m\ s^{-1}$ )
$c_p$	specific heat capacity ( $J\ kg^{-1}\ K^{-1}$ )	$\Delta p$	total pressure difference between the chimney base and the ambient or pressure loss of a component (Pa)
$d$	pipe diameter (m)	<i>Greek symbols</i>	
$D$	chimney diameter (m)	$\gamma$	lapse rate of temperature ( $K\ m^{-1}$ )
$f$	wall friction factor 0.008428	$\delta$	thickness (m)
$g$	gravitational acceleration ( $m\ s^{-2}$ )	$\varepsilon$	pressure loss coefficient
$G$	solar radiation ( $W\ m^{-2}$ )	$\eta$	energy conversion efficiency (%)
$h$	altitude (m)	$\lambda$	conductive heat transfer coefficient ( $W\ m^{-1}\ K^{-1}$ )
$H$	chimney height (m)	$\rho$	density ( $kg\ m^{-3}$ )
$l$	pipe length (m)	<i>Subscripts</i>	
$\dot{m}$	mass flow rate of hot air passing through the chimney ( $kg\ s^{-1}$ )	c	chimney
$Nu$	Nusselt number	coll	collector
$P_{out}$	electric power generated by the turbines (W)	f	friction or fluid
$Pr$	Prandtl number	in	chimney inlet
$Q$	heat output ( $J\ s^{-1}$ )	Max	maximum
$R_{coll}$	collector radius (m)	out	exit
$Re$	Reynolds number	t	turbine
$T$	temperature (K)	w	wall
$U$	total heat transfer coefficient from chimney air-flow to atmospheric air ( $W\ m^{-2}\ K^{-1}$ )	$\infty$	ambient
$U_{\infty}$	convective heat transfer coefficient between the chimney wall and the airflow inside the solar chimney ( $W\ m^{-2}\ K^{-1}$ )	$\infty in$	collector inlet
$U_f$	convective heat transfer coefficient between the chimney wall and atmospheric air ( $W\ m^{-2}\ K^{-1}$ )		

date, humans have no experience in constructing gigantic towers more than 1000 m high. Many high or sky-high-level mountains are distributed in the world. The relative heights from the top to the bottom of the mountains reach thousands of meters. As far as the special topographical feature is concerned, a combined solar chimney power plant with a collector covering the mountain feet, a concrete tower constructed on an adjacent large-relatively-

height mountain, and a penstock crawling the mountain to connect them up is a good design for a solar chimney power plant [19,20]. Both the concrete tower and the leaning penstock produce ‘chimney’ effect for the Schailch’s classical solar chimney power plant prototype. The total vertical height of the tower and the leaning penstock is just equal to the ‘chimney’ height for the Schailch’s classical prototype. Floating solar chimney power technology, another innovative solar power technology, was developed by Papageorgiou [21]. The floating solar chimney can also reach multi-km heights. Therefore, to find out the optimal ‘chimney’ height (i.e. the optimal altitude of mountain where tower can be constructed or the optimal length of the floating solar chimney) for a finite collector is significant for obtaining the highest energy conversion efficiency.

In this paper, a detailed investigation of solar chimney power plant using differential method is carried out. The maximum chimney height for convection and the optimal chimney height for maximum power output are presented and analyzed. Finally, the performances of several-mega-watt solar chimney power plants are investigated.

## 2. Theoretical model

Solar chimney power system is a thermal power generating system. The energy conversion in the power system can

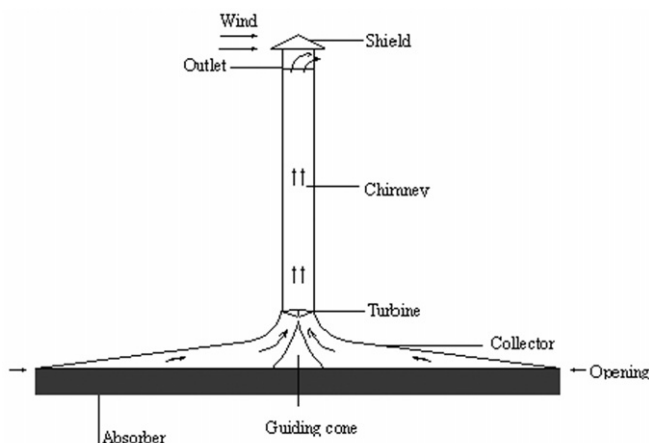


Fig. 1. Schematic diagram of solar chimney power generating system.

be divided into three phases: the collector converts solar energy to heat energy of air; the chimney which acts as a thermal engine drives hot air through the turbine generators which in turn convert airflow in form of kinetic energy to electric power. Here, a detailed theoretical model is developed to evaluate the performance of solar chimney power system. The analysis is based on the following four assumptions:

1. The air follows the ideal gas law.
2. Only the buoyancy force is considered in the chimney.

The solar chimney is the actual thermal engine of the power system. The chimney converts the hot airflow into kinetic energy which is actually determined by the temperature rise of the collector outlet airflow and the chimney height.

The pressure difference,  $\Delta p$ , which is produced between the chimney base and the ambient, is calculated by

$$\Delta p = g \int_0^H (\rho_\infty(h) - \rho(h)) dh \quad (1)$$

where  $g$  is the gravitational acceleration of air;  $\rho_\infty(h)$  and  $\rho(h)$  are the density of air at any altitude  $h$  inside the chimney and outside the chimney, respectively.

The physical properties of air are assumed to vary linearly with air temperature because of the low temperature range encountered. Air density  $\rho$  and air specific heat capacity  $c_p$  can be taken to be related by empirical relation for air properties between 300 and 350 K [22] and is given by

$$\rho = 1.1614 - 0.00353(T - 300) \quad (2)$$

$$c_p = (1.007 + 0.00004(T - 300)) \cdot 10^3 \quad (3)$$

Combining Eqs. (1) and (2),  $\Delta p$  can be further written as

$$\begin{aligned} \Delta p &= 0.00353 \cdot g \int_0^H (T(h) - T_\infty(h)) dh \\ &= 0.00353 \cdot g \\ &\cdot \left( H \cdot T(H) - \int_0^H dT(h) - \int_0^H T_\infty(h) dh \right) \end{aligned} \quad (4)$$

Considering the effect of the gradual lapse of atmospheric air temperature,  $T_\infty(h)$  is given by

$$T_\infty(h) = T_{\infty in} - \gamma_\infty h \quad (5)$$

where  $T_{\infty in}$  is the temperature of atmospheric air at the collector inlet;  $\gamma_\infty$  is the lapse rate of atmospheric air temperature.

When heat loss through the chimney wall is considered,  $T(h)$  is given by

$$\begin{aligned} -c_p \dot{m} dT(h) &= U(T(h) - T_\infty(h)) \pi D dh + \dot{m} g dh \\ &= \pi D U T(h) dh + \pi D U \gamma_\infty h dh \\ &\quad + (\dot{m} g - \pi D U T_{\infty in}) dh \end{aligned} \quad (6)$$

since the variation of airflow kinetic energy is negligible when air rises by  $dh$ . Here,  $D$  is the chimney diameter;  $\dot{m}$  denotes the mass flow rate of hot air passing through the chimney, and can be calculated with the following equation:

$$\dot{m} = \rho_{in} A_c V_{in} \quad (7)$$

where  $A_c$  is the cross section area of chimney;  $\rho_{in}$  is the density of the chimney inlet airflow;  $V$  is the rate of the chimney inlet airflow.  $U$  is total heat transfer coefficient from chimney airflow to atmospheric air and can be expressed as

$$U = 1/(1/U_f + \delta/\lambda + 1/U_\infty) \quad (8)$$

where  $\delta$  is the thickness of chimney wall;  $\lambda$  is the conductive heat transfer coefficient of concrete used for the wall construction;  $U_\infty$  denotes the convective heat transfer coefficient between the chimney wall and ambient wind and  $U_f$  denotes the convective heat transfer coefficient between the chimney wall and the flow. Table 1 shows correlations employed for forced convection coefficients of a flow vertically across a pipe and a flow in a pipe [23].

The boundary condition for Eq. (6), is that the temperature of the chimney inlet airflow, is equal to temperature of the collector outlet airflow, which is mathematically given by

$$T(0) = T_{\infty in} + \frac{\pi G \eta_{coll}}{c_p \dot{m}} R_{coll}^2 \quad (16)$$

where  $G$  is solar radiation;  $\dot{Q}$  is heat output of hot air;  $R_{coll}$  is the collector radius;  $\eta_{coll}$  is collector efficiency.

From Eqs. (6) and (8),  $T(h)$  can be further written as

$$\begin{aligned} T(h) &= T_{\infty in} - \gamma_\infty h - \frac{\dot{m}(g - \gamma_\infty c_p)}{\pi D U} \\ &\quad + e^{-\frac{\pi D U}{c_p \dot{m}} h} \left( \frac{\pi G \eta_{coll}}{c_p \dot{m}} R_{coll}^2 + \frac{\dot{m}(g - \gamma_\infty c_p)}{\pi D U} \right) \end{aligned} \quad (17)$$

So,  $T(H)$  can also be written as

$$\begin{aligned} T(H) &= T_{\infty in} - \gamma_\infty H - \frac{\dot{m}(g - \gamma_\infty c_p)}{\pi D U} \\ &\quad + e^{-\frac{\pi D U}{c_p \dot{m}} H} \left( \frac{\pi G \eta_{coll}}{c_p \dot{m}} R_{coll}^2 + \frac{\dot{m}(g - \gamma_\infty c_p)}{\pi D U} \right) \end{aligned} \quad (18)$$

From Eqs. (2)–(10),  $\Delta p$  can be further expressed as

$$\begin{aligned} \Delta p &= 0.00353 \cdot g H \cdot \left( \frac{\pi D U + \dot{m} g}{2 c_p \dot{m}} H - \frac{1}{2} \gamma_\infty H - \frac{\dot{m}(g - \gamma_\infty c_p)}{\pi D U} \right) \\ &\quad + T_{\infty in} + e^{-\frac{\pi D U}{c_p \dot{m}} H} \left( \frac{\pi G \eta_{coll}}{c_p \dot{m}} R_{coll}^2 + \frac{\dot{m}(g - \gamma_\infty c_p)}{\pi D U} \right) \end{aligned} \quad (19)$$

When heat loss through the chimney wall is not considered,  $T(h)$  takes the form,

$$-c_p \dot{m} dT(h) = \dot{m} g dh \quad (20)$$

Combining Eqs. (8) and (18),  $T(h)$  becomes,

$$T(h) = T_{\infty in} - \frac{g}{c_p} h + \frac{\pi G \eta_{coll}}{c_p \dot{m}} R_{coll}^2 \quad (21)$$

Table 1  
Correlations employed for forced convection adopted by Xu et al. [23]

		Flow source
<i>For a flow vertically sweeping across a pipe exterior</i>		
		$5 \leq Re < 10^3$
$Nu = 0.44Re^{0.5}$	(9)	
		$10^3 \leq Re < 2 \times 10^5$
$Nu = 0.22Re^{0.6}$	(10)	
		$2 \times 10^5 \leq Re \leq 2 \times 10^6$
$Nu = 0.02Re^{0.8}$	(11)	
<i>For a flow in a pipe</i>		$Re \leq 2200$
$Nu = 1.86 \left( Re \cdot Pr \frac{d}{l} \right)^{1/3} \left( \frac{\mu_f}{\mu_w} \right)^{0.14}$	(12)	$2200 \leq Re < 10^4$
$Nu = 0.0214(Re^{0.8} - 100)Pr^{0.4} \left( 1 + \left( \frac{d}{l} \right)^{2/3} \right) \left( \frac{T_f}{T_w} \right)^{0.45}$	(13)	$10^4 \leq Re \leq 1.2 \times 10^5$ and $l/d \geq 60$
$Nu = 0.023Re^{0.8}Pr^{0.3}$	(14)	$10^4 \leq Re \leq 1.2 \times 10^5$ and $l/d < 60$
$Nu = 0.023 \left( 1 + \left( \frac{d}{l} \right)^{0.7} \right) Re^{0.8} Pr^{0.3}$	(15)	

and  $T(H)$  also becomes

$$T(H) = T_{\infty in} - \frac{g}{c_p} H + \frac{\pi G \eta_{coll}}{c_p \dot{m}} R_{coll}^2 \quad (22)$$

$\Delta p$  can also be rewritten as

$$\Delta p = 0.00353 \cdot gH \cdot \left( \frac{\pi G \eta_{coll}}{c_p \dot{m}} R_{coll}^2 - \frac{g}{2c_p} H + \frac{1}{2} \gamma_{\infty} H \right) \quad (23)$$

The pressure difference  $\Delta p$  is usually caused by friction loss  $\Delta p_f$  in the chimney, entrance loss  $\Delta p_{in}$ , exit kinetic energy loss  $\Delta p_{out}$ ,  $\Delta p_t$  being used to transfer to the kinetic energy of the turbine [15]. Thus,

$$\Delta p = \Delta p_t + \Delta p_f + \Delta p_{in} + \Delta p_{out} \quad (24)$$

where

$$\Delta p_f = f \frac{H}{D} \frac{1}{2} \rho V^2 \quad (25)$$

$$\Delta p_{in} = \varepsilon_{in} \frac{1}{2} \rho V^2 \quad (26)$$

$$\Delta p_{out} = \varepsilon_{out} \frac{1}{2} \rho_{out} V_{out}^2 \quad (27)$$

The pressure loss coefficients are recommended as the wall friction factors  $f = 0.008428$  chimney [24], entrance loss coefficient  $\varepsilon_{in} = 0.056$  by assuming inlet guide vane angle and collector roof height are respectively  $22.5^\circ$  and  $0.356^\circ$  [25], and exit kinetic energy loss coefficient  $\varepsilon_{out} = 1.058$  [26].

$\Delta p$  is finally solved combining Eqs. (7), (23)–(27).

The electric power generated by the turbine generators,  $P_{out}$ , can be expressed as

$$P_{out} = \eta_{tg} \Delta p_t \cdot V \cdot A_c \quad (28)$$

where  $\eta_{tg}$  is the efficiency of turbine generators.

Total energy conversion efficiency can be expressed as the ratio of  $P_{out}$  to solar radiation input on the collector

$$\eta = \frac{P_{out}}{\pi R_{coll}^2 G} \quad (29)$$

### 2.1. Maximum chimney height

The static pressures at the inlet and the outlet of the chimney are nearly equal to the static pressure at the same height in the ambient, respectively. Assuming the linear variation of the pressure, the pressure of air at any height in the chimney is nearly equal to that at the same height in the ambient. So, density difference between the air flow in the chimney and the ambient at any height depends on the temperature difference.

Temperature of air reduces more quickly than the air in the surroundings due to heat transfer to gravitational potential and heat loss through chimney wall when flowing along the chimney. However, the temperature of the air at the chimney outlet should not lower than the temperature of the air at the same height in the surroundings. Or else, according to the state equation, the density of air flow at the chimney outlet is higher than the corresponding density

of the air in the surroundings because of the same pressure. This counteracts a part of buoyancy, decelerating airflow through the solar chimney. This therefore results in a maximum chimney height  $H_{Max}$  for a given collector. For the critical combination, the temperature of chimney outlet air  $T(H_{Max})$  is equal to that of the atmospheric air  $T_{\infty}(H_{Max})$  around the chimney outlet. This is given by

$$T(H_{Max}) = T_{\infty}(H_{Max}) \quad (30)$$

in compact form. Explicitly written out, it becomes

$$\begin{aligned} T_{\infty} - \gamma_{\infty} H_{Max} - \frac{\dot{m}(g - \gamma_{\infty} c_p)}{\pi DU} \\ + e^{-\frac{\pi DU}{c_p \dot{m}} H_{Max}} \left( \frac{\pi G \eta_{coll} R_{coll}^2}{c_p \dot{m}} + \frac{\dot{m}(g - \gamma_{\infty} c_p)}{\pi DU} \right) \\ = T_{\infty} - \gamma_{\infty} H_{Max} \end{aligned} \quad (31)$$

The resulting expression for  $H_{Max}$  is

$$H_{Max} = \frac{c_p \dot{m}}{U \pi D} \cdot \ln \left( \frac{\pi^2 U D G \eta_{coll} R_{coll}^2}{c_p \dot{m}^2 (g - \gamma_{\infty} c_p)} + 1 \right) \quad (32)$$

$\Delta p$  and  $H_{Max}$  are finally solved with Matlab combining Eqs. (7), (23)–(27), (32).

### 3. Validation

To validate the theoretical model, the calculated results are compared with the measurements in the Manzanares prototype which had a 244 m diameter collector and a chim-

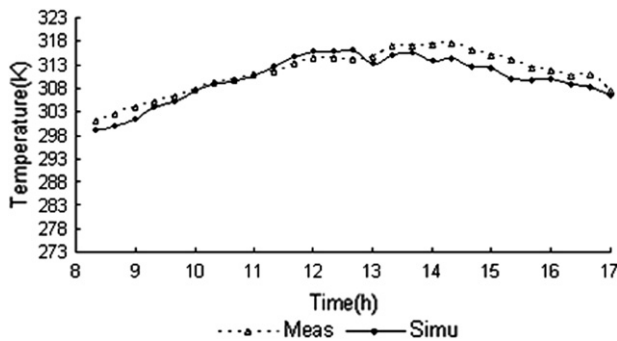


Fig. 2. Airflow temperature in chimney during the day (September 2, 1982).

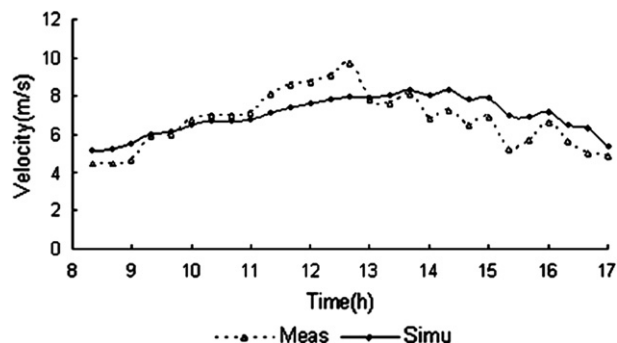


Fig. 3. Airflow velocity in chimney during the day (September 2, 1982).

ney 194.6 m tall, 0.00125 m in metallic wall thickness and 10.16 m in diameter. The values of the performance including air temperature rise and velocity in the chimney are calculated with the theoretical model based on the measurements [2] which is also used to calculate collector efficiency and compared with the corresponding measurements during daytime on September 2, 1982, as shown in Figs. 2 and 3.

As shown in Figs. 2 and 3, during daytime, an agreement for temperature rise and airflow velocity in the chimney is good. It is concluded that the theoretical model is reasonably valid for solar chimney power system.

### 4. Results and discussion

The study is carried out based on the Manzanares prototype solar chimney power plant. In the steady analyses in the paper, the collector efficiency is assumed to be a constant at 31.3% i.e. mean efficiency of the collector measured in the Manzanares plant [2], and solar radiation is selected as the maximum measured value of  $1040 \text{ W m}^{-2}$  from June to September, in 1987 [2]. In fact, air density is influenced by temperature and local atmospheric pressure. Different atmospheric pressure changing at different sites will result in different maximum height. Fig. 4 shows the comparison of  $H_{Max}$  under different atmospheric pressures and using empirical relation as expressed with Eq. (2). In the figure, with an increase in atmospheric pressure from 90 kPa to 101.325 kPa, maximum height decreases slightly from 777.2 m to 788.8 m. An agreement within a difference of 1.3% between all the  $H_{Max}$  under different atmospheric pressures and using empirical relation is obtained. Especially,  $H_{Max}$  under atmospheric pressure of 100 kPa is nearly equal to that using empirical relation. So, the influence of atmospheric pressure on  $H_{Max}$  is negligible. The static pressure variation along height and that lessened due to the dynamic pressure, which is negligible compared with the magnitude of atmospheric pressure, is not included in the model.

The dry adiabatic lapse rate of air temperature is around  $0.0098 \text{ K m}^{-1}$  inside the chimney (or slightly higher, if

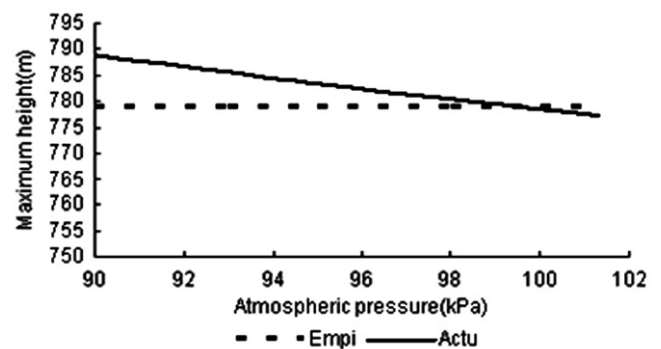


Fig. 4. Comparison of  $H_{Max}$  under different actual atmospheric pressures and using empirical relation.

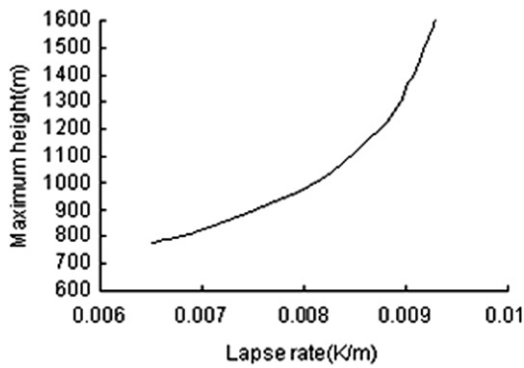


Fig. 5. Variation of  $H_{Max}$  with different lapse rate of atmospheric air temperature.

there is heat loss through the chimney walls) [11], but is variable outside the chimney at different time at different sites [27]. The standard lapse rate of atmospheric temperature is around  $0.0065 \text{ K m}^{-1}$  [28]. Also, the lapse rate of atmospheric temperature may be close to the dry adiabatic value. Fig. 5 gives the variation of maximum height with lapse rate of atmospheric temperature. In the figure, maximum height gradually increases with the lapse rate increasing, and go to infinity at around  $0.0098 \text{ K m}^{-1}$ . It is concluded that high chimney is suitable to be constructed at dry atmospheric conditions. The standard value of  $0.0065 \text{ K m}^{-1}$  is used kept for the lapse rate of atmospheric temperature in the following analysis.

The calculated power outputs for the concrete chimneys with different wall thickness from 0.0001 m to 0.8 m, originally 0.00125 m-thickness metallic wall chimney, and adiabatic chimney are shown in Fig. 6.

Average temperature lapse rate of airflow in the original metallic chimney are calculated to be  $0.01067 \text{ }^\circ\text{C/m}$ , which is higher than that in the adiabatic chimney, due to heat loss across chimney wall when hot air flows along the chimney. It is far more than the standard atmospheric temperature lapse rate. A maximum height for hot air convection where airflow temperature is usually equal to atmospheric temperature therefore exists. This also results in a maximum chimney height  $H_{Max}$  for a given collector, just equal to the maximum height for hot air convection. Fig. 6 shows

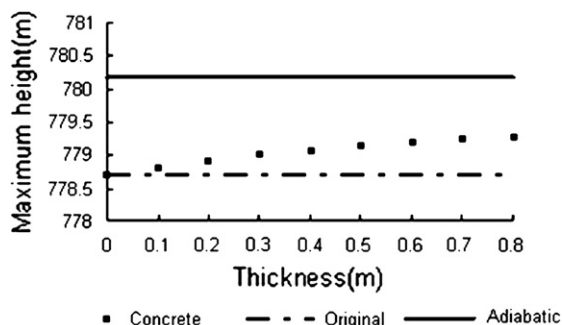


Fig. 6. Comparison of  $H_{Max}$  for different-thickness concrete wall chimneys, original metallic chimney, and adiabatic chimney.

$H_{Max}$  for different-thickness concrete wall chimneys, original metallic chimney, and adiabatic chimney for 244 m diameter collector keeping the ratio of height to cross section of chimney constant as 19.15 when solar radiation is  $1040 \text{ W m}^{-2}$ . In the figure, the maximum  $H_{Max}$  is observed for adiabatic chimney, being 9 m higher than the corresponding value for original metallic chimney.  $H_{Max}$  increases logarithmically with the increase from 0.0001 m to 0.8 m in the thickness of concrete chimney wall. There is dependence on heat loss across the thickness of the chimney wall. The results show that chimney wall with large thickness and low heat conductive coefficient helps increase of  $H_{Max}$ .

Fig. 7 shows variation of power output with chimney height from 100 m to  $H_{Max}$  of 778.7 m. In the figure, an increase of chimney height from 100 m to 778.7 m, also translates to a power output initially from 28.9 kW to a maximum 102.2 kW and finally to 92.3 kW for  $H_{Max}$ . The power output corresponding to  $H_{Max}$  is not the maximum power output for the solar chimney power plant. In the simple analysis, mean density of airflow in the chimney can be thought to be a constant resulting from small temperature range. So,  $P_{out}$  is only directly proportional to  $\Delta P \cdot \dot{m}$ . The increase of chimney height helps increase  $\dot{m}$ . This leads to the reduction of  $\Delta P$ . Fig. 8 shows variations of mass flow rate and pressure difference with chimney height from 100 m to 778.7 m. In the figure, the optimal power output is not at 100 m or at 615 m, but at a chimney height between 100 m and 778.7 m, as shown in Fig. 7.

As shown in Fig. 7, there is the optimal chimney height  $H_{Opt}$  of 615 m for obtaining the maximum power output of

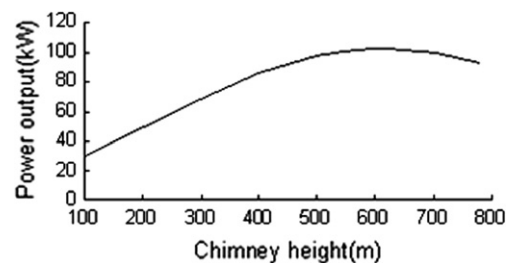


Fig. 7. Variation of power output with chimney height.

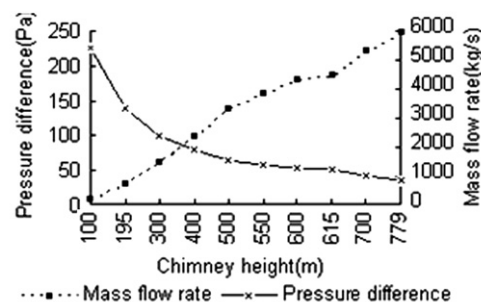


Fig. 8. Variations of mass flow rate and pressure difference with chimney height.

102.2 kW. Compared with  $H_{Max}$ ,  $H_{Opt}$  is suitable for construction reducing the chimney height by about 163 m.

Solar energy is the energy source of solar chimney power plant. So, solar radiation influences  $H_{Max}$  and  $H_{Opt}$ . Fig. 9 shows variations of  $H_{Max}$  and  $H_{Opt}$  and the corresponding power outputs with solar radiation from  $200 \text{ W m}^{-2}$  to  $1000 \text{ W m}^{-2}$ . As shown in Fig. 9, both  $H_{Max}$  and  $H_{Opt}$  increase with increase in solar radiation, and the power output difference between them also increases from 2.7 kW to 20.9 kW. For the regions with ordinary solar radiation between  $400 \text{ W m}^{-2}$  and  $800 \text{ W m}^{-2}$ , average chimney height of about 500 m based on the Manzanares prototype is suitable for deriving the maximum power output to large extent.

Compared with other renewable energy utilizing systems, an advanced merit of solar chimney power system, which is considered to have the most potential in solving the energy crisis, is to that solar chimney power plants can produce electric power on a large-scale. It is very significant to evaluate the performance of large-scale solar chimney power plant. Generally, the ratio of height to cross section of chimney for large-scale solar chimney power plant should not be large [1] with the consideration of large pressure losses and difficulty to robust engineering. In related work, Schlaich et al. [14] designed a 100 MW power plant which had a 1000 m tall chimney with a 110 m diameter and a 200 MW power plant which had a 1000 m tall chimney with a 120 m diameter. Von Backström and Gannon [11] investigated the performance of a 200 MW power plant with a 1500 m height and a 160 m diameter. In order to evaluate the performance of solar chimney power plant, conveniently, the ratio of height to cross section of chimney is kept to at 9 in the analysis. The thickness of the reinforced concrete walls decreases from 0.99 m at the inlet to 0.25 m at the outlet for the 1000 m tall chimney designed by Schlaich [29]. The mean thickness for the reinforced concrete walls from the inlet to the outlet of chimney is kept at a constant of 0.62 m for convenient calculation in the analysis.

Fig. 10 shows variations of  $H_{Max}$  and  $H_{Opt}$  and the corresponding power outputs with solar collector radius. As expected, there are larger  $H_{Max}$  and  $H_{Opt}$  for larger collector areas, receiving more solar radiation. Also, correspond-

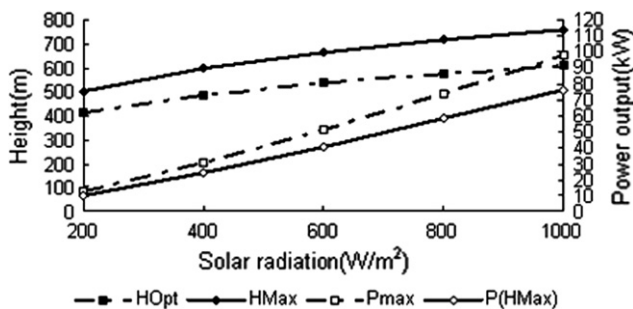


Fig. 9. Variations of  $H_{Max}$  and  $H_{Opt}$  and the corresponding power outputs with solar radiation.

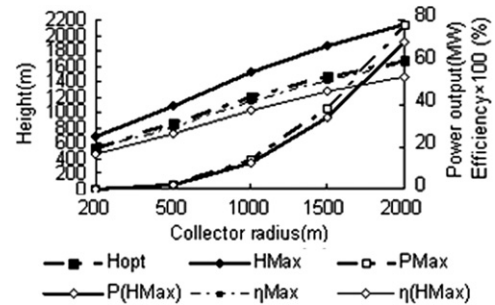


Fig. 10. Variations of  $H_{Max}$  and  $H_{Opt}$  and the corresponding power outputs with solar collector radius.

ing maximum efficiency increases from 0.18% to 0.59% with collector radius of 200 m to 2000 m. Since that the solar chimney power plant essentially is a solar thermal power generating plant receiving heat from a heat source at relatively low temperature. The process of energy conversion is restricted by the laws of thermodynamic.

## 5. Conclusions

In this paper, the maximum chimney height for convection and the optimal chimney height for maximum power output are presented and analyzed based on the Manzanares prototype using a theoretical model validated with the measurements of the only one prototype in Manzanares. With respect to a special collector, negative buoyancy at the latter chimney will occur if chimney height is more than the maximum height. The power plant would obtain the maximum energy conversion efficiency if chimney height is equal to the optimal height. To find out the optimal chimney height for a collector covered at finite ground is significant for the decision-making in determining the dimensions for construction. The following conclusions can be drawn from the analyses.

- (1) The accuracy of the theoretical model in predicting the maximum chimney height over the range of atmospheric pressure from 90 kPa to 101.3 kPa is estimated. An agreement within a difference of 1.3% between all the  $H_{Max}$  under different atmospheric pressures and using empirical relation is obtained. This shows the influence of atmospheric pressure on  $H_{Max}$  is negligible.
- (2) As standard lapse rate of atmospheric temperature is used, the maximum power output of 102.2 kW is obtained for the optimal chimney height of 615 m, which is lower than the maximum chimney height with a power output of 92.3 kW.
- (3) The influence of various lapse rates of atmospheric temperatures on maximum height is analysed. The maximum height gradually increases with the lapse rate increasing and go to infinity at a value of around  $0.0098 \text{ K m}^{-1}$ . It is concluded that high chimney is suitable to be constructed at dry atmospheric conditions.

- (4) Analyses of several-mega-watt power plants show that the maximum height for convection and optimal height for maximum power output increase with larger collector.

### Acknowledgements

This research was supported by the Excellent Doctoral Thesis Foundation of Huazhong University of Science and Technology (HUST), the Youth Chenguang Projects of Science and Technology of Wuhan City of China under Grant No. 20015005037 and No. 20055003059-34, and Natural Science Foundation of Hubei Province under Grant No. 2005ABA047.

### References

- [1] J. Schlaich, *The Solar Chimney*, Edition Axel Menges, Stuttgart, Germany, 1995.
- [2] W. Haaf, Solar chimneys part II: preliminary test results from Manzanares Pilot Plant, *Int. J. Sol. Energy* 2 (1984) 141–161.
- [3] R.J.K. Krisst, Energy transfer system, *Alternat. Sources Energy* 63 (1983) 8–11.
- [4] H.A. Kulunk, Prototype solar convection chimney operated under humid conditions, in: T.N. Veiroglu (Ed.) *Proceedings of the 7th Miami International Conference on Alternative Energy Sources*, vol. 162, 1985.
- [5] N. Pasumarthi, S.A. Sherif, Experimental and theoretical performance of a demonstration solar chimney model, Part II: experimental and theoretical results and economic analysis, *Int. J. Energy Res.* 22 (1998) 443–461.
- [6] X.P. Zhou, J.K. Yang, B. Xiao, G.X. Hou, Experimental study of temperature field in a solar chimney power setup, *Appl. Therm. Eng.* 27 (2007) 2044–2050.
- [7] N. Pasumarthi, S.A. Sherif, Experimental and theoretical performance of a demonstration solar chimney model-Part I: mathematical model development, *Int. J. Energy Res.* 22 (1998) 277–288.
- [8] M.A.K. Lodhi, Application of helio-aero-gravity concept in producing energy and suppressing pollution, *Energy Convers. Manage.* 40 (1999) 407–421.
- [9] M.A. dos S Bernardes, A. Vob, G. Weinrebe, Thermal and technical analyzes of solar chimneys, *Sol. Energy* 75 (2003) 511–524.
- [10] M.A. dos S Bernardes, R.M. Valle, M.F. Cortez, Numerical analysis of natural laminar convection in a radial solar heater, *Int. J. Therm. Sci.* 38 (1999) 42–50.
- [11] T.W. Von Backström, A.J. Gannon, Compressible flow through solar power plant chimneys, *ASME J. Sol. Energy Eng.* 122 (2000) 138–145.
- [12] A.J. Gannon, T.W. von Backström, Solar chimney turbine performance, *ASME J. Sol Energy Eng.* 125 (1) (2003) 101–106.
- [13] H. Pastohr, O. Kornadt, K. Gurlebeck, Numerical and analytical calculations of the temperature and flow field in the upwind power plant, *Int. J. Energy Res.* 28 (2004) 495–510.
- [14] J. Schlaich, R. Bergermann, W. Schiel, G. Weinrebe, Design of commercial solar updraft tower systems-utilization of solar induced convective flows for power generation, *ASME J. Sol. Energy Eng.* 127 (2005) 117–124.
- [15] E. Bilgen, J. Rheault, Solar chimney power plants for high latitudes, *Sol. Energy* 79 (2005) 449–458.
- [16] J.P. Pretorius, D.G. Kröger, Critical evaluation of solar chimney power plant performance, *Sol. Energy* 80 (2006) 535–544.
- [17] N. Ninic, Available energy of the air in solar chimneys and the possibility of its ground-level concentration, *Sol. Energy* 80 (2006) 804–811.
- [18] F.N. Onyango, R.M. Ochieng, The potential of solar chimney for application in rural areas of developing countries, *Fuel* 85 (2006) 2561–2566.
- [19] X.P. Zhou, J.K. Yang, B. Xiao, X.D. Yuan, Current study status and application potential of solar chimney thermal power systems in China, in: *Proceedings of World Renewable Energy Congress, Conference Proceedings*, Florence, Italy, August 2006.
- [20] D. Bonnelle, *Solar Chimney, Water Spraying Energy Tower, and Linked Renewable Energy Conversion Devices: Presentation, Criticism and Proposals*. Doctoral thesis, University Claude Bernard-Lyon 1, France, July, 2004, Registration Number: 129-2004.
- [21] C. Papageorgiou, Solar turbine power stations with floating solar chimneys, in: *IASTED Proceedings of Power and Energy Systems, EuroPES 2004, Conference*, Rhodes Greece, July 2004, pp. 151–158.
- [22] K.S. Ong, C.C. Chow, Performance of a solar chimney, *Sol. Energy* 74 (2003) 1–17.
- [23] G.L. Xu, X.M. Wang, T.H. Wu, W.H. Chen, *Engineering Heat Transfer*, China Electric Power Press, Beijing, China, 2005.
- [24] F.M. White, *Fluid Mechanics*, fourth ed., McGraw-Hill, 1999.
- [25] C.F. Kirstein, T.W. von Backström, Flow through a solar chimney power plant collector-to-chimney transition section, *J. Sol. Energy Eng.* 128 (2006) 312–317.
- [26] T.W. Von Backström, A. Bernhardt, A.J. Gannon, Pressure drop in solar power plant chimneys, *J. Sol. Energy Eng.* 125 (2003) 165–169.
- [27] S.Z. Zhou, R.Y. Zhang, C. Zhang, *Meteorology and Climatology*, third ed., Higher Education Press, Beijing, China, 1997.
- [28] H.Z. Zhao, *Engineering Fluid Mechanics*, Huazhong University of Science and Technology Press, Wuhan, China, 2005.
- [29] J. Schlaich, Tension structures for solar electricity generation, *Eng. Struct.* 21 (1999) 658–668.